ISSN 1674-1056
http://cpb.iphy.ac.cn
http://iopscience.iop.org/cpb
中国物理 B
Chinese Physics
中国物理
Chinese Physics B

Investigation of convergent Richtmyer-Meshkov instability at tin/xenon interface with pulsed magnetic driven imploding

Shaolong Zhang(张绍龙), Wei Liu(刘伟), Guilin Wang(王贵林), Zhengwei Zhang(章征伟), Qizhi Sun(孙奇志), Zhaohui Zhang(张朝辉), Jun Li(李军), Yuan Chi(池原), Nanchuan Zhang(张南川)

Citation: Chin. Phys. B . 2019, 28(4): 044702. **doi:** 10.1088/1674-1056/28/4/044702
Journal homepage: http://cpb.iphy.ac.cn; http://iopscience.iop.org/cpb

What follows is a list of articles you may be interested in

Property of slice square polycapillary x-ray optics

Shi-Qi Peng(彭诗棋), Zhi-Guo Liu(刘志国), Tian-Xi Sun(孙天希), Kai Wang(王锴), Long-Tao Yi(易龙涛), Kui Yang(杨魁), Man Chen(陈曼), Jin-Bang Wang(王金榜)

Chin. Phys. B . 2016, 25(2): 024102. **doi:** 10.1088/1674-1056/25/2/024102

Polycapillary X-ray lens for secondary focusing Beijing synchrotron radiation source

Li Yu-De, Lin Xiao-Yan, Liu Shi-Gang, He Jin-Long, Guo Fei, Sun Tian-Xi, Liu Peng

Chin. Phys. B . 2013, 22(4): 044103. **doi:** 10.1088/1674-1056/22/4/044103

Investigation of convergent Richtmyer–Meshkov instability at tin/xenon interface with pulsed magnetic driven imploding*

Shaolong Zhang(张绍龙), Wei Liu(刘伟)†, Guilin Wang(王贵林), Zhengwei Zhang(章征伟), Qizhi Sun(孙奇志), Zhaohui Zhang(张朝辉), Jun Li(李军), Yuan Chi(池原), and Nanchuan Zhang(张南川)

Institute of Fluid Physics, China Academy of Engineering Physics, Mianyang 621900, *China*

(Received 28 December 2018; revised manuscript received 29 January 2019; published online 19 March 2019)

The Richtmyer–Meshkov instability at the interface of solid state tin material and xenon gases under cylinder geometry is studied in this paper. The experiments were conducted at FP-1 facility in Institute of Fluid Physics, China Academy of Engineering Physics (CAEP). The FP-1 facility is a pulsed power driver which could generate high amplitude magnetic field to drive metal liner imploding. Convergent shock wave was generated by impacting a magnetic-driven aluminium liner onto a inner mounted tin liner. The convergent evolution of the disturbance pre-machined onto the tin liner's inner surface was diagnosed by x-radiography. The spike amplitudes were derived from x-ray frames and were compared with linear theory. An analytical model containing material strength effect was derived and matched well to the experimental results. This sensibility of the disturbance evolution to material strength property shines light to the application of Richtmyer–Meshkov instability to infer material strength.

Keywords: Richtmyer–Meshkov instability, pulsed power driver, convergent shock wave

PACS: 47.20.Ma, 41.50.+h, 46.40.Cd **DOI:** 10.1088/1674-1056/28/4/044702

1. Introduction

When a shock wave passes through an interface of different density materials, disturbances on the interface will experience instability growing which is known as the Richtmyer–Meshkov instability (RMI). Understanding the characteristics of this phenomenon is of great importance in a wide range of scientific and engineering applications among which the instability encountered in inertial confinement fusion (ICF)[1,2] is of great interest. During the past 20 years, considerable amounts of analytical, computational, and experimental works dealt with the planar version of this problem.[3,4] It is benefit to focus on the basic physical process underlying the onset and development of the RMI in simple geometries. Many aspects that affect the RMI behavior have been studied thoroughly under planer configuration, such as the Mach number effects,[5,6] the initial condition effects,[7,8] the Atwood number effects,[9,10] the non-equilibrium characteristics,[11] and so on. However, the imploding of the ICF capsule is in convergent geometry which cannot be investigated by the planner shock wave.[12] In convergent geometry, the RMI differs from the planar case due to the geometrical effects on the instability which has been already recognized and studied by theoretical and numerical methods.[13–19] The experimental study, however, is very limited. To better understand the dynamics of the RMI in convergent geometry and validate models in such configuration, sufficient experimental data are needed. Recently, some researchers are working hard to generate convergent shock wave in shock tubes.[20,21] Holder *et al.*[22] reported laboratory experiments with a convergent shock tube, using a detonable gas mixture to produce a cylindrically convergent shock. But, such a device is lack of flexibility due to the use of explosive gas. Zhai *et al.*,[23] Apazidis *et al.*,[24] and Biamino *et al.*[25] have experimentally proven the possibility of generating a converging cylindrical shock wave using a conventional shock tube. Most of the experiments studied RMI behavior at gas/gas interface. In this paper, however, we present an alternative way using magnetic driving method to generate convergent shock wave in solid materials and study the RMI of solid/gas interface.

The RM instability phenomena have been thoroughly studied for perfect fluid and gases. Recently, however, the RM instability in solid materials is of growing interest.[18,26–28] In materials with strength, the RMI growth is arrested and stabilized at an amplitude which is in inverse proportion to yield stress Y.[29] Dimonte *et al.*[30] developed a model for the strength suppression of the RMI that can be used to infer yield strength under shock loading. The RMI has also been adopt to explain the ejecta phenomenon in solid materials. Buttler *et al.*[31] developed an ejecta source term model that links to the surface perturbations of shocked materials. The RMI evolution was also recommended as an alternative method for evaluating the viscosity of metals. Mikaelian[32] presented an analytical expression for the amplitude of perturbations at the interface of two viscous fluids and found a relation between fluid viscosity and solid strength. Besides the above upcom-

*Project supported by the National Natural Science Foundation of China (Grant Nos. 11605183 and 11502254).

†Corresponding author. E-mail: liuisbad@hotmail.com

© 2019 Chinese Physical Society and IOP Publishing Ltd

ing applications (all of which are in planner regime), the RMI in solid materials under convergent geometry has also critical effect on some engineering applications.[33–35] With the above motivation, a series of experiments were conducted to investigate the convergent RMI phenomenon at the interface between solid tin material and xenon gas in this paper.

2. Methods

In solid materials shock waves are mostly produced by impacting. A variety of driven methods exist, such as projectile of gun type, explosive systems, electrical, electromagnetic, and combined accelerators, devices on the basis of radiation sources (laser radiation and x-radiation, electron, and ion beams, *etc*.). The method of impactor driven by magnetic field pressure possesses a number of important advantages:

(i) Absence of action of explosive products on the liner means a possibility of its inertial convergence, excludes additional weakly controlled influence on the target, and eliminates a necessity to take this additional action into account during numerical analysis.

(ii) A possibility to set the current pulse of required shape, *i.e*., the availability of a broad range of characteristics of the impactor drive, a possibility to obtain different impact velocities.

(iii) High symmetry of loading conditioned by the method of magnetic field generation and absence of additional factors (for example, HE initiation system or non-uniformity of laser radiation).

(iv) "transparency" of the magnetic field allows recording the velocity not only of the inner but also the outer surface of the impactor.

With so much advantages, we choose magnetic-driven liner-on-target method to generate shock waves in the tin material. A general magnetically driven cylinder liner-on-target shock experiment is shown in Fig. 1. For an axial directed current I, passing through a liner of radius R, an azimuthal directed magnetic filed B, produces a driving pressure given by

$$P = \frac{\mu_0 I^2}{8\pi^2 R^2}. \tag{1}$$

The FP-1 facility (Fig. 2) is a pulsed power generator consisting of 216 capacitors located at Institute of Fluid Physics, CAEP. This facility can deliver a peak current of 2 MA to the load with a 7-μs rise time at charging voltage of ±20 kV. The details of the facility can be referred to Ref. [36]. A ϕ30-mm inner diameter aluminium liner with 0.5-mm thickness can be driven to a velocity of about 1 km/s (when inner surface diameter is ϕ18 mm) under this current amplitude.[37,38] Figure 3 shows the load configuration of FP-1 facility for the RMI experiment setup. shock wave is generated by impact of the magnetic driven aluminium liner onto the inner mounted tin target. The inner diameter of the liner is 30 mm and the thickness of the liner is 0.5 mm. The target is a 21-mm inner diameter and 0.7-mm thick tin cylinder. Sinusoidal perturbations with mode number of 21 were machined on the inner surface of the target. Peak to valley amplitude of the perturbation is 0.5 mm. Equation (2) shows the mathematical expression of the perturbation.

$$r(\theta) = 10.25 + 0.25\sin(21\theta), \theta \in [0, 2\pi]. \tag{2}$$

The volume between liner and target was pumped to vacuum to avoid retardation from the gases in this zone. Figure 4 shows the cross section of the impactor and target liner.

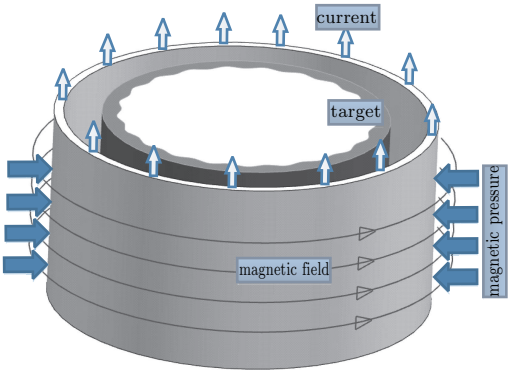


Fig. 1. Scheme of liner-impactor driven by magnetic field.

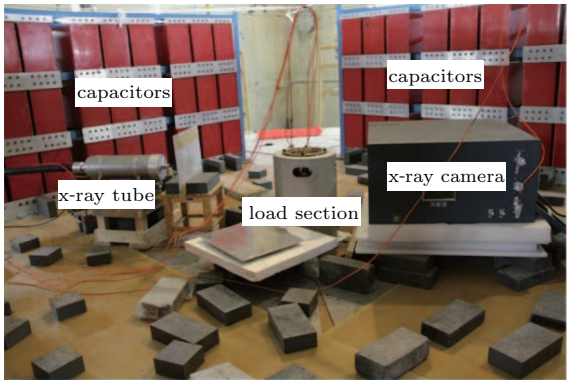


Fig. 2. FP-1 facility.

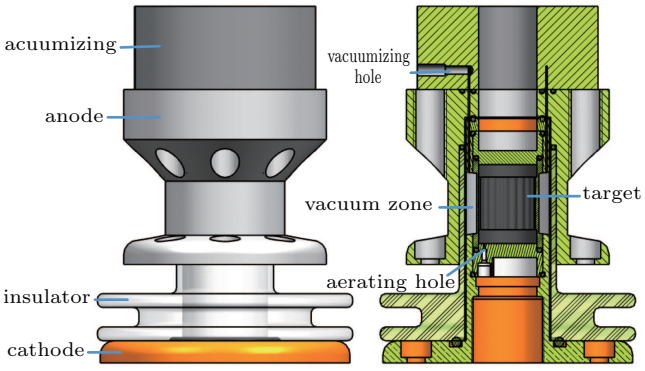


Fig. 3. Load configuration of the FP-1 facility.

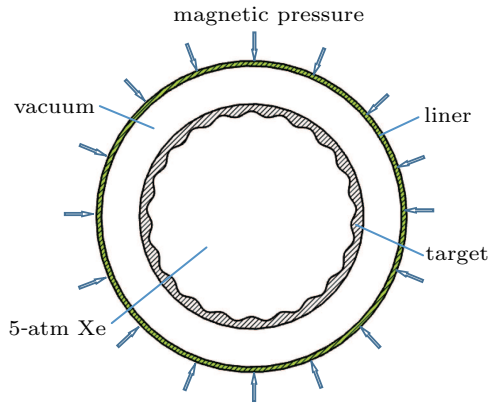


Fig. 4. Cross section of the impactor and target liner.

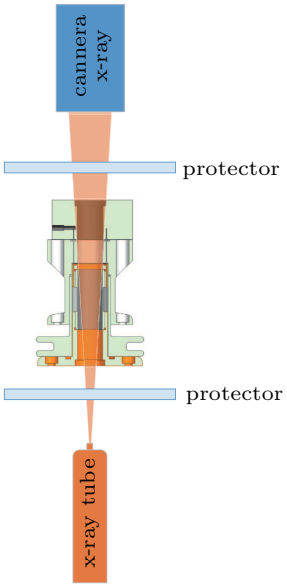


Fig. 5. Scheme of the radiography system.

The impacting condition on the tin target was derived from velocity history of the inner surface which were measured with a smooth tin liner before the RMI experiment. A DISAR velocimetry system[39] was used to obtain the velocity history. Rogowski coil was mounted in the load section of the FP-1 facility to collect the current data passing through the liner. A 1D MHD code[40] in cylindrical coordinate regime was used to analysis the liner imploding procedure with the current data as input condition. Inner surface velocity history was compared between the code's prediction and experiment's measurement, which will validate the code. Then the impact condition was inferred by the validated code.

Radiography is the main diagnostic for this RMI experiment. It allows the visualization of the disturbance evolution in the otherwise inaccessible target interior during the course of the experiment. The x-ray source size is 1 mm to 1.5 mm with about a 50-ns pulse duration. A Marx bank with charge voltage of 46 kV delivered about 450-kV peak voltage to the x-ray diodes which could generate about 5.2×10^{-6} C/kg x-ray at 1-m distance. X-ray film was collected by a high-resolution CCD camera after a fluorescent screen. Both the x-ray diode and camera were carefully protected from high speed fragments along the axial orientation. Figure 5 shows the arrangement of the radiography system.

3. Results and discussion

3.1. Impact condition

Before the RMI experiment, a velocity measurement experiment was conducted to provide free surface velocity data for 1D MHD code validation and impact condition determination. Figure 6 shows the target configuration used for velocity measurement experiment. Two mini-holes were machined on the target liner which made the DISAR laser probe accessible to the light reflected by the outer impactor liner. Figure 7 shows the velocity measurement results. It can be seen that both the impactor and target liner inner surface velocity history were obtained. The significant jump at 11.5 μs in the impactor velocity curve is induced by mass ejection from the mini-hole when the impactor liner contacted with the target liner. The impact velocity is 1 km/s. Figure 8 gave the comparison of the impactor liner velocity between the one-dimensional (1D)

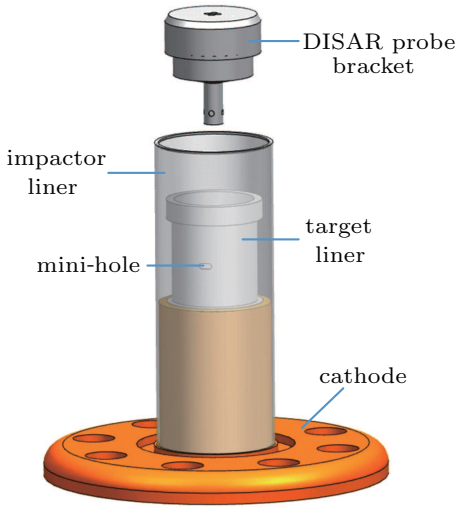


Fig. 6. Target configuration for velocity measurement.

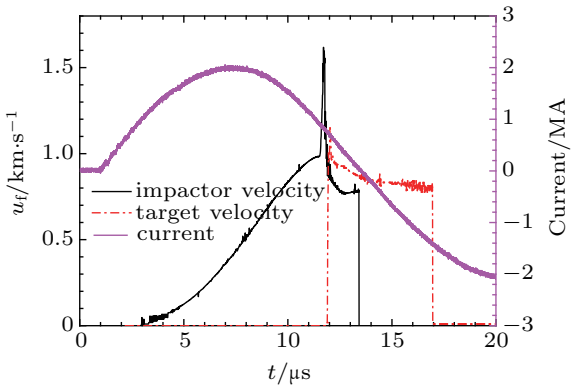


Fig. 7. Velocity measurement results.

MHD code calculation and experimental data which shows excellent agreement. Then, with the validated code we can derive that the impact pressure is 9.75 GPa and shock velocity is 3.22 km/s in the tin target. Under this condition the tin target is still in solid state.

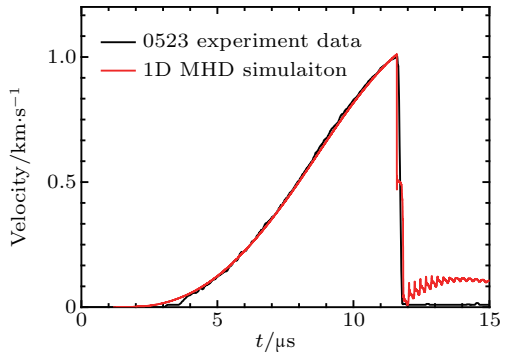


Fig. 8. Impactor velocity comparison between 1D MHD simulation and experiment data.

3.2. Repeatability of driving condition

The radiography Marx bank generate only one pulse in one shot which means only one figure could be obtain in one shot. However, to study RMI problem we need a time series pictures. So, sequent shots should be conducted with the same driving condition which demand a perfect discharging repeatability of the facility. The repeatability property of the FP-1 facility were examined and verified before the RMI experiment. Figure 9(a) shows the current comparison between two shots and figure 9(b) shows the impactor velocity comparison between two individual shots. Great repeatability can be inferred from these pictures.

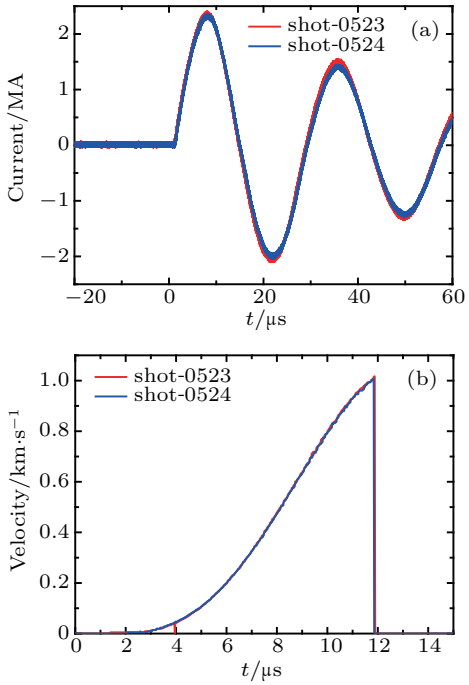


Fig. 9. Repeatability property of the FP-1 facility: (a) current comparison and (b) velocity comparison.

3.3. RMI experiment

After the above preparation, a series of RMI experiment were conducted and axial radiography figures (shown in Fig. 10) at four individual dynamic times were obtained. Here, the time is relative to the current start time in the circuit. The top two pictures show the initial static frame and the comparison between the 18.3-μs dynamic frame and the initial disturbance profile (the white disturbance curve). From this comparison we can note that the spikes developed from valley zone of the initial disturbance which infer that the disturbance phase already reversed at 18.3 μs.

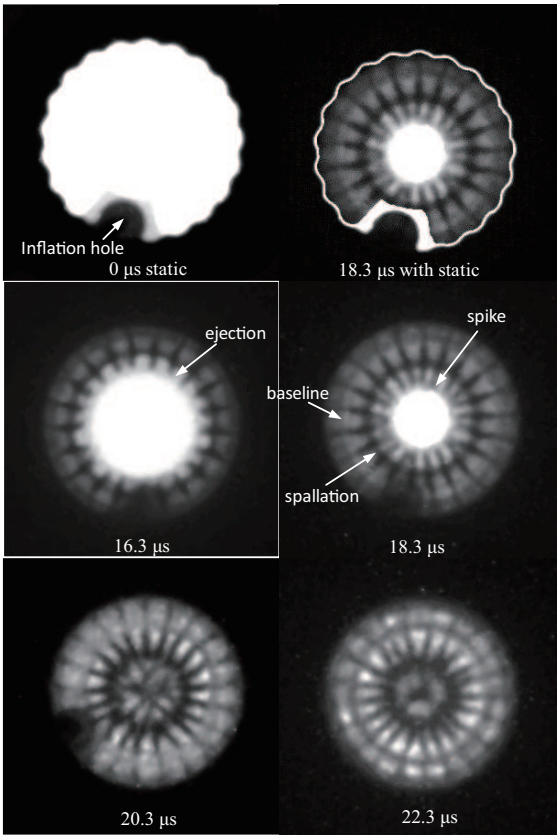


Fig. 10. Axial radiography pictures of the RMI experiment.

It is interesting that there exist disturbance growings on both sides of the target although initially the disturbance machined only on the inner surface. We believe that it is belong to the spallation of the target which would induce disturbance on the other side. Figure 11 shows the Radiographic frame of a smooth tin target (without disturbance) from side view. It can be seen clearly that there exist spallation phenomenon in the tin target which confirmed the suppose above.

It can be note from the dynamic frames in Fig. 10 that there exists shadow zone ahead and between the disturbance spikes. This phenomenon belongs to the micro-ejection of the tin target surface which is induced by not perfectly smooth surface. The inner surface of the tin target was machined using line-cutting method which limited the surface roughness is

about 3.2 micrometer rms. The radius of the interface (spallation)'s and spike peak's position at each time were summarized in Table 1 excepted for the last two frames whose spikes were contacting each other.

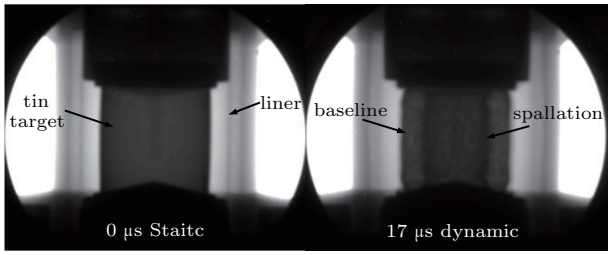


Fig. 11. Radial radiography pictures of smooth target.

Table 1. Radii of the spallation, spike peaks and spike amplitude derived from x-ray frames.

Time/μs	Spallation/mm	Spike peak/mm	Spike amplitude/mm
16.3	6.9	5.7	1.2
18.3	5.1	3.4	1.7
20.3	–	–	–
22.3	–	–	–

3.4. Discussion of strength effect

An analytical model for the disturbance evolution in cylindrical geometry was given by Mikaelian[41] under some assumptions of incompressible, irrotational, and inviscid flows with perturbations in linear regime. The governing equation is shown in below

$$\frac{\mathrm{d}^2\eta}{\mathrm{d}t^2}+2\frac{\dot{R}}{R}\frac{\mathrm{d}\eta}{\mathrm{d}t}-(nA-1)\frac{\ddot{R}}{R}\eta=0, \tag{3}$$

where R is he cylinder radius, n is the mode number of the perturbation, and $A=(\rho_2-\rho_1)/(\rho_2+\rho_1)$ is the Atwood number. A "dot" over a letter refers to the time derivation. Just as what Richtmyer[42] has done, we assume the interface moves with constant velocity ($R=R_0-\Delta v t$) after shock breaking out which is represented as an impulsive acceleration $\ddot{R}=\Delta v\delta(t)$. Then an analytical solution to Eq. (3) can be derived.

$$\eta(t)=\eta_0\left[1+(nA-1)\left(1-\frac{R_0}{R}\right)\right]. \tag{4}$$

From the measurement of the interface radius's convergence rate in Fig. 10, we can obtain the interface moving velocity Δv which is about 800 m/s. Spike amplitude was also measured from Fig. 10 which is shown in Fig. 12 together with results Eq. (4) and Margolin's surface area conservation model. It can be noted that Margolin's surface area conservation model did not capture the phase inverting phenomenon at all and differed a lot from experimental results even qualitatively. It can also be seen from Fig. 12 the model of Eq. (3) predicts a higher growing value than experimental results. Main reason for this discrepancy is the absence of strength effect in the model of Eq. (3) which is known as an suppression to the disturbance growing. In fact, the impact pressure in our experiment is much lower than tin's molten pressure which is above 33 GPa. So, the strength effect must be considered in the model.

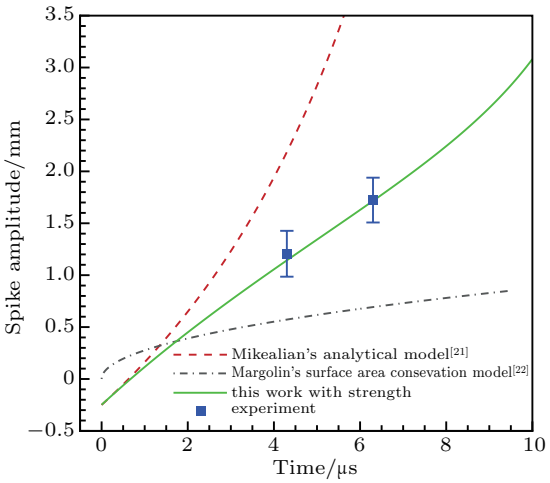


Fig. 12. Spike amplitude evolution comparison between experiment and analytical model result.

Mikaelian[32] analyzed the viscous effect on shock-induced interface instability in planner geometry and derived the governing equation. He found some similarity between metal strength and fluid viscous under the following relation:

$$Y=\frac{2}{3}\dot{\eta}_0 k\mu, \tag{5}$$

where Y is metal strength, μ is fluid viscous, k is wave number of disturbance, and $\dot{\eta}_0$ is the disturbance growth rate immediately after the passage of the shock. Under impulsive acceleration assumption, as Richtmyer[42] showed, $\dot{\eta}_0$ can be written as

$$\dot{\eta}_0=\eta_0\Delta v k A. \tag{6}$$

With this relation, we can derive the governing equation for disturbance evolution containing strength effect in planner geometry.

$$\frac{\mathrm{d}^2\eta}{\mathrm{d}t^2}+\frac{3Y}{\eta_0\Delta v\rho_0}\frac{\mathrm{d}\eta}{\mathrm{d}t}-gkA\eta=0. \tag{7}$$

Similarly, supposing the strength effect is an intrinsic property of materials which means it has no relationship with configuration, the governing equation in cylinder geometry with strength effect becomes:

$$\frac{\mathrm{d}^2\eta}{\mathrm{d}t^2}+\left(\frac{3Y}{\eta_0\Delta v\rho_0}+2\frac{\dot{R}}{R}\right)\frac{\mathrm{d}\eta}{\mathrm{d}t}-(nA-1)\frac{\ddot{R}}{R}\eta=0. \tag{8}$$

Equation (8) was solved numerically (details given in Appendix A), the result is shown in Fig. 12. It can be seen clearly

in Fig. 12 that the spike amplitude growth with strength effect matches well to experimental results which means strength property indeed has critical effect on the disturbance growth rate in our experiment.

4. Conclusion

A series of RMI experiments in solid tin material were initiated on FP-1 facility. Shock wave was generated by magnetic driving method for its advantage in lots of aspects. The 1D MHD code predicted well the impactor velocity which means that the driving condition could be derived from this code and also the desired impact condition could be designed beforehand using this code. With the limitation that the radiography diagnostic could only generate one pulse in one shot, excellent repeatability property of the FP-1 facility guarantees the reliability of the RMI experiment in our study. Five individual times of the disturbance development were obtained by radiography. The spikes of the disturbance existed in both sides of the target which maybe induced by spallation of the tin target on impact. The amplitude of the spikes is derived from the radiographic frames and compared with linear analytical model. The model containing strength effects shows excellent agreement to experimental results. This conclusion makes confidence to the application of using the Richtmyer–Meshkov instability to infer material strength. The results in this paper have validated the magnetic driving method which is appropriate for studying the solid state RMI problem. But lack of sufficient time interval frames makes the results dissatisfy. So, much individual time of the disturbance development will be investigated in the future.

Appendix A: Solving method for Eq. (8)

Under impulse assumption, as Richtmyer[42] showed, the $\ddot{R}$ can be written as:

$$\ddot{R} = \Delta v \delta(t - t_{\rm s}),$$

where $t_{\rm s}$ is the time of shock arrival and Δv is the jump in velocity after shock arrival. Substitute this formula into Eq. (8) and integrate over $[t_{s_-}, t_{s_+}]$. Where $t_{s_\pm}$ are times immediately before and after shock arrival. Considering $\dot{R} = 0$ at this time interval and assuming the strength has no effect during this shock passing process, we can obtain:

$$\dot{\eta}_+ = \dot{\eta}_- + (nA - 1)\frac{\eta_{\rm s}}{R_{\rm s}}\Delta v,$$

where $\dot{\eta}_-$ and $\dot{\eta}_+$ are the growth rates immediately before and after the passage of the shock, $\eta_{\rm s}$ is the amplitude at shock arrival time, and $R_{\rm s}$ is the radius at that time. For an initially stationary interface we have $\dot{\eta}_- = 0$, $\eta_{\rm s} = \eta_0$, and $R_{\rm s} = R_0$. Assuming a shock arriving at $t_{\rm s} = 0$, then equation (8) becomes the following initial value problem

$$\begin{cases} \dfrac{{\rm d}^2\eta}{{\rm d}t^2} + \left(\dfrac{3Y}{\eta_0 \Delta v \rho_0} + 2\dfrac{\dot{R}}{R}\right)\dfrac{{\rm d}\eta}{{\rm d}t} = 0, \\ \eta\,|_{t=0} = \eta_0, \\ \dot{\eta}\,|_{t=0} = (nA-1)\dfrac{\eta_0}{R_0}\Delta v. \end{cases} \tag{A1}$$

Equation (A1) can be solved numerically using Runge–Kutta method. We choose strength parameter of tin as the static one $Y = 12$ MPa, and $\rho_0 = 7.28$ g/cm^3, $A = 1$, $\Delta v = 800$ m/s, $n = 21$.

Acknowledgment

The authors would thank Yuesong Jia, Xiaoming Zhao and Weidong Qin for their kindly help to maintain the FP-1 facility. The authors would also thank Yang Zhang, Zheng Fu and Lili Wang for their fruitful discussion of the experiment results.

References

[1] Dittrich T R, Hammel B A, Keane C J, McEachern R, Turner R E, Haan S W and Suter L J 1994 *Phys. Rev. Lett.* **73** 2324
[2] Clark D S, Haan S W, Cook A W, Edwards M J, Hammel B A, Koning J M and Marinak M M 2011 *Phys. Plasmas* **18** 082701
[3] Brouillette M 2002 *Ann. Rev. Fluid Mech.* **34** 445
[4] Prestridge K, Orlicz G, Balasubramanian S and Balakumar B J 2013 *Phil. Trans. R Soc. A* **37** 20120165
[5] Orlicz G C, Balakumar B J, Tomkins C D and Prestridge K P 2009 *Phys. Fluids* **21** 064102
[6] Yang J, Wan Z H, Wang B F and Sun D J 2015 *Chin. Phys. Lett.* **32** 034701
[7] Thornber B, Drikakis D, Youngs D L and Williams R J R 2010 *J. Fluid Mech.* **654** 99
[8] Mariani C, Vandenboomgaerde M, Lourdan G, Souffland D and Houas L 2008 *Phys. Rev. Lett.* **100** 254503
[9] Tao Y S, Wang L F, Ye W H, Zhang G C, Zhang J C and Li Y J 2012 *Acta Phys. Sin.* **61** 075207 (in Chinese)
[10] Jourdan G and Houas L 2005 *Phys. Rev. Lett.* **95** 204502
[11] Chen F, Xu A G and Zhang G C 2018 *Phys. Fluids* **30** 102105
[12] Wang L F, Ye W H, He X T, Wu J F, Fan Z F, Xue C, Guo H Y, Miao W Y, Yuan Y T, Dong J Q, Jia G, Zhang J, Li Y J, Liu J, Wang M, Ding Y K, and Zhang W Y 2017 *Sci. China-Phys. Mech. Astron.* **60** 055201
[13] Zhang Q and Graham M J 1997 *Phys. Rev. Lett.* **79** 2674
[14] Matsuoka C and Nishihara K 2006 *Phys. Rev. E* **74** 066303
[15] Tian B L, Fu D X and Ma Y W 2006 *Acta Mech. Sin.* **22** 9
[16] Lombardini M 2008 Richtmyer Meshkov Instability in Converging Geometries, Ph.D. Dissertation (Pasadena: California Institute of Technology)
[17] Guo H Y, Yu X J, Wang L F, Ye W H, Wu J F and Li Y J 2014 *Chin. Phys. Lett.* **31** 044702
[18] Liu J, Feng Q J and Zhou H B 2014 *Acta Phys. Sin.* **63** 155201 (in Chinese)
[19] Liang Y, Guan B, Zhai Z G and Luo X S 2017 *Acta Phys. Sin.* **66** 064701 (in Chinese)
[20] Biamino L, Jourdan G, Mariani C, Houas L, Vandenboomgaerde M and Souffland D 2015 *Exp. Fluids* **56** 26
[21] Luo X S, Ding J C, Wang M H, Zhai Z G and Si T 2015 *Phys. Fluids* **27** 091702
[22] Holder D A, Smith A V, Barton C J and Youngs D L 2003 *Laser Part. Beams* **21** 403
[23] Zhai Z G, Si T, Luo X S, Yang J M, Liu C L, Tan D W and Zou L Y 2012 *Phys. Fluids* **24** 026101

[24] Apazidis N, Kjellander and Tillmark N 2013 *Shock Waves* **23** 361

[25] Biamino L, Jourdan G, Mariani C, Houas L, Vandenboomgaerde M and Souffland D 2014 *J. Fluids Eng.* **136** 091204

[26] Piriz A R, Lóez Cela J J and Tahir N A 2009 *Nucl. Instrum. Method A* **606** 139

[27] Piriz A R, Lóez Cela J J and Tahir N A 2009 *Phys. Rev. E* **80** 046305

[28] Yin J W, Pan H, Wu Z H, Hao P C, Duan Z P and Hu X M 2017 *Acta Phys. Sin.* **66** 204701 (in Chinese)

[29] Piriz A R, Lóez Cela J J, Tahir N A and Hoffmann D H H 2008 *Phys. Rev. E* **78** 056401

[30] Dimonte G, Terrones G, Cherne F J, Germann T C, Dupont V, Kadau K, Buttler W T, Oro D M, Morris C and Preston D L 2011 *Phys. Rev. Lett.* **107** 264502

[31] Buttler W T, Oró D M, Preston D L, Mikaelian K O, Cherne F J, Hixson R S, Mariam F G, Morris C, Stone J B, Terrones G and Tupa D 2012 *J. Fluid Mech.* **703** 60

[32] Mikaelian K O 2013 *Phys. Rev. E* **87** 031003

[33] Rousculp C L, Oro D M, Margolin L G,Griego J R, Reinovsky R E and Turchi P J 2015 *Tech. Rep. LA-UR*-15-26264, Los Alamos National Laboratory

[34] Rousculp C L, Oro D M, Griego J R, Turchi P J, Reinovsky R E, Bradley J T, Cheng B, Freeman M S and Patten A R 2016 *Tech. Rep. LA-UR*-16-21901, Los Alamos National Laboratory

[35] Rousculp C L, Oro D M, Griego J R, Patten A R, Neukirch L P, Reinovsky R E, Turchi P J, Bradley J T, Reass W A, Fierro F, Saunders A, Mariam F G, Freeman M S, Cheng B and Tang Z 2017 *Tech. Rep. LA-UR*-17-23974, Los Alamos National Laboratory

[36] Yang L B, Sun C W, Liao H D and Hu X J 2002 *High Power Laser and Particle Beams* **14** 767

[37] Zhang Z W, Wei Y, Sun Q Z, Liu W, Zhao X M, Zhang Z H, Wang G L, Guo S and Xie W P 2016 *High Power Laser and Particle Beams* **28** 045017 (in Chinese)

[38] Zhang S L, Zhang Z W, Sun Q Z, Liu W, Zhao X M, Zhang Z H, Wang G L and Jia Y S 2017 *High Power Laser and Particle Beams* **29** 105002 (in Chinese)

[39] Weng J D, Tan H, Wang X, Ma Y, Hu S L and Wang X S 2006 *Appl. Phys. Lett.* **89** 111101

[40] Zhang Y, Dai Z H, Sun Q Z, Zhang Z W, Sun H Q, Wang P, Ding N, Xue C, Wang G Q, Shen Z J, Li X and Wang J G 2018 *Acta Phys. Sin.* **67** 080701 (in Chinese)

[41] Mikaelian K O 2005 *Phys. Fluid* **17** 094105

[42] Richtmyer R D 1960 *Commun. Pure Appl. Math.* **13** 297